The 2025 World Congress on
Advances in Structural Engineering and Mechanics (ASEM25)
BEXCO, Busan, Korea, August 11-14, 2025

Principal Stress Rotation in Geotextile Encased Sand During Cyclic Loading

Hyeong-Joo Kim[1] Voltaire Anthony Corsino[2] Hyeong-Soo Kim[3]
James Vincent Reyes[4] Tae-Wong Park[5] Tae-Eon Kim[6], So-Hyi Jung[7]

1) Department of Civil Engineering, Kunsan National University, Gunsan 54150, Republic of Korea
2), 4), 6), 7) Department of Civil and Environmental Engineering, Kunsan National University, Gunsan 54150, Republic of Korea
3), 5) Renewable Energy Research Institute, Kunsan National University, Gunsan 54150, Republic of Korea

[2]vacorsino@kunsan.ac.kr

ABSTRACT

This study investigates stress direction changes and reinforcement behavior in geotextile-encased sand specimens subjected to cyclic triaxial loading. During axial loading, applied forces are redistributed radially through the soil matrix and mobilized as tensile stresses in the encasing geotextile fabric. At the particle level, stress orientation evolves along the principal axes, with rearrangement occurring during cyclic shearing. Results show that prolonged loading leads to progressive rearrangement and softening of the soil matrix, accompanied by a reduction in confinement efficiency due to fabric loosening at the soil–fabric structure. Additionally, post-cyclic reconsolidation tests reveal that the reinforcement retains its structural function, maintaining sufficient confinement and supporting partial recovery of the soil skeleton. These findings highlight the dynamic interaction between fabric tension and internal soil structure, and demonstrate that encasement continues to provide mechanical benefits on reconsolidation.

1. INTRODUCTION

Geotextile encasement has emerged as an effective solution for improving the cyclic performance of soils, especially in earthquake-prone or wave-affected environments. By providing lateral confinement, geotextile fabrics enhance the stiffness and strength of soil, reduce deformation, and delay pore pressure buildup during cyclic loading (Yoo & Abbas, 2019; Miranda et al., 2017). This method has been widely applied in stone columns, geotextile tube embankments, and sandbag foundations installed in soft or saturated ground conditions (Raithel et al., 2002; Kim et al., 2023). Although the mechanical benefits of encasement are well-documented, limited research has explored the internal stress redistribution and principal stress rotation that occur during repeated loading. As cyclic loads are applied, soil particles undergo progressive rearrangement and potential softening, affecting the mobilization of tensile forces in the geotextile. In

---

1 Professor
2, 4, 6, 7Graduate Student
3, 5 Ph. D.

dense specimens, this confinement effect tends to activate at higher strains, while in looser soils, it can engage earlier due to rapid lateral expansion. The dynamic coupling between particle behavior and fabric tension remains poorly understood, particularly under undrained principal stress conditions.

Furthermore, the role of post-cyclic reconsolidation in restoring soil strength and density within encased systems is also an area of interest. Studies such as Ishihara and Yoshimine (1992) and Green (2001) have shown that cyclic liquefaction and subsequent reconsolidation lead to significant densification, yet the effect of geotextile encasement on this process remains underexplored.

This study aims to investigate the evolution of internal stresses, confinement mobilization, and reconsolidation behavior in geotextile-encased sand specimens subjected to cyclic loading. By focusing on principal stress rotation and post-cyclic performance, this work contributes to a deeper understanding of fabric-soil interactions and provides insights for the design of resilient geosynthetic-reinforced systems.

2. EXPERIMENTAL PROGRAMME

Specimen preparation and experimental set up:

The test specimens were prepared using sand collected from Saemangeum Port, South Korea. The material had a fines content of 14% and median particle size D50=0.14mm. Based on criteria established by Seed et al. (1985) and Youd and Idriss (2001), the soil was classified as potentially liquefiable under undrained cyclic loading. Cylindrical specimens (70 mm diameter × 140 mm height) were prepared at two target relative densities namely loose 35% and medium dense 50%. The moist tamping method (Ladd, 1978; Frost & Park, 2003) was employed to achieve the target densities. For the encased specimens, a flexible woven polyester (PET) geotextile was used. The fabric was pre-cut and positioned inside the mold prior to tamping, ensuring full encasement. Un-encased specimens were also prepared as controls for comparison.

The experimental setup, including the dynamic triaxial system and visualization of the encased specimen with labeled parts, is shown in Fig. 1. Tests were performed using a dynamic triaxial apparatus (Wille Geotechnik, Germany). Axial load was measured using an internal load cell, and displacement was captured using an LVDT connected to the loading rod. A volume-pressure controller (VPC) was used to regulate confining and back pressures. Data were acquired and processed using the Geosys software suite.

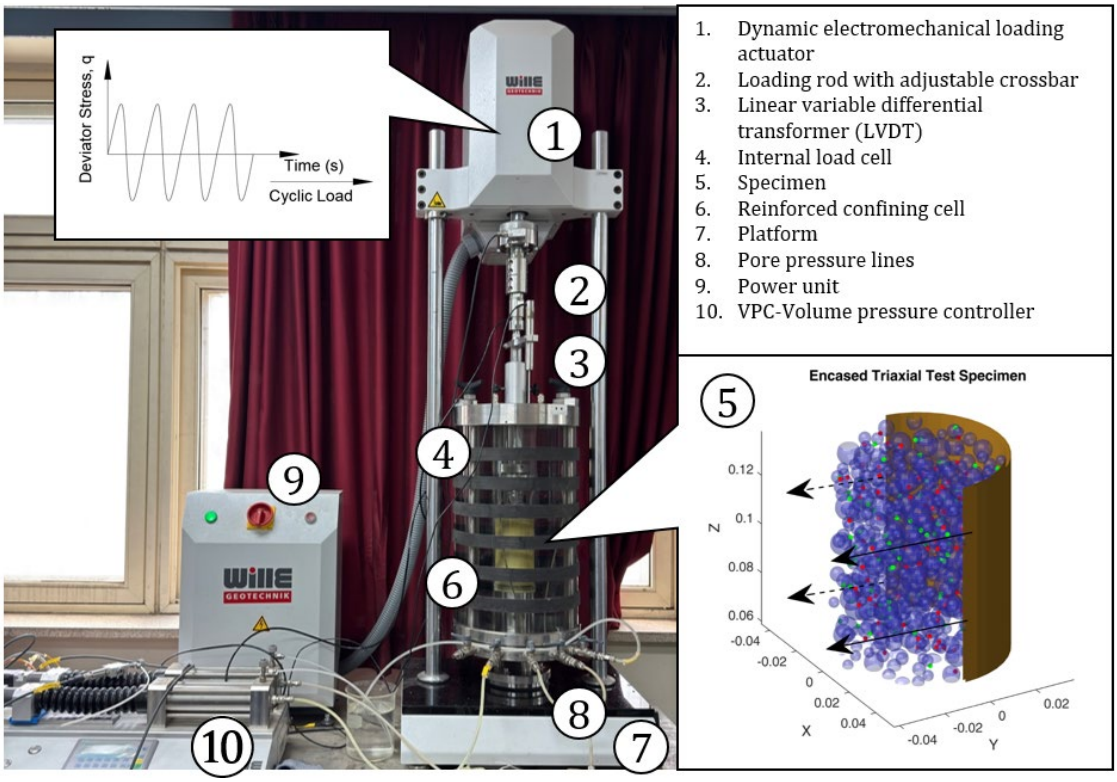

Fig. 1 Experimental Set up

Cyclic Loading Programme:

Cyclic triaxial tests were performed in accordance with ASTM D5311M-13 under undrained conditions. All specimens were isotropically consolidated to an effective confining pressure of 100 kPa. Cyclic axial loads were applied at a frequency of 0.1 Hz, replicating quasi-static loading while minimizing inertial effects (Zhu et al., 2021). Applied Cyclic Stress Ratios (CSR) range from 0.15 to 0.30 with 0.05 increments. The failure criteria were defined as pore pressure ratio R_u =1.0 or double amplitude axial strain DA = 5%, whichever is achieved first. Visualization of the encased specimen's integrity during cyclic loading is shown in Fig. 2(a), while Fig. 2(b) provides a photograph of the specimen prior to installation in the triaxial chamber.

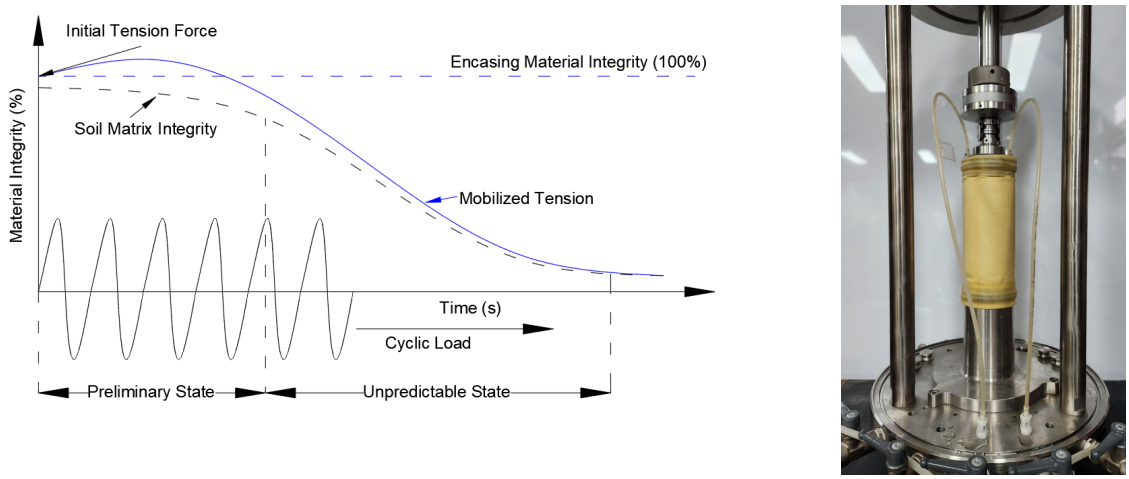

(a) (b)

Fig. 2 (a) Visualization of specimen integrity and (b) specimen set up.

Post Cyclic Loading Programme:

The applied loading program, including the post-cyclic reconsolidation stage, is summarized in Fig. 3(a). After the cyclic phase, the drainage valve was opened to allow pore pressure dissipation and specimen reconsolidation under drained conditions. The process was considered complete once the volume change stabilized and effective stress recovered. Subsequently, drained monotonic shearing was performed at a constant strain-rate to evaluate the residual strength. A representative specimen in its loosened, reconsolidated state is shown in Fig. 3(b). Volumetric strain measurements were used to compute the final relative density, enabling evaluation of cyclic densification effects.

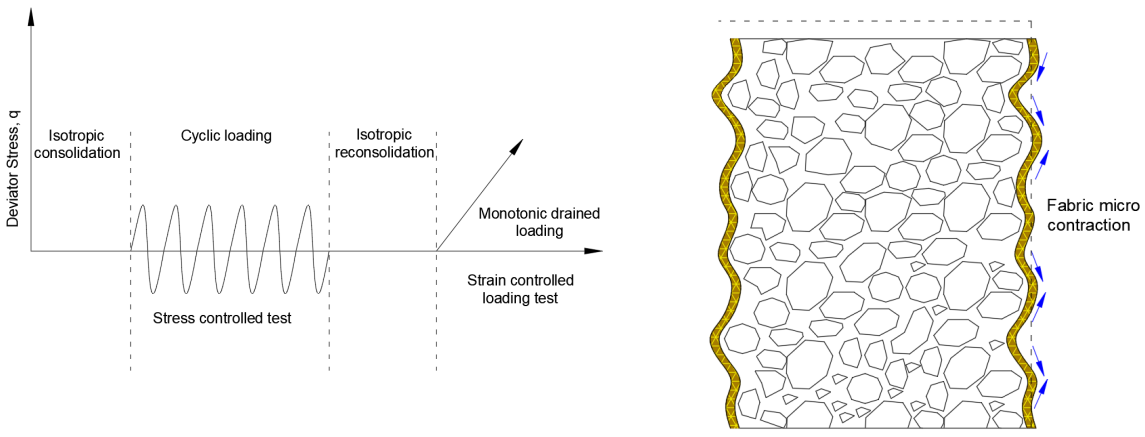

(a) (b)

Fig. 3 (a) Loading programme and (b) reconsolidated state visualization.

3. RESULTS AND DISCUSSION

Cyclic resistance and pore pressure response:

Geotextile encasement significantly enhanced the cyclic resistance of the sand specimens compared to un-encased controls. As shown in Fig. 4(a), PET-encased specimens endured a higher number of cycles before reaching failure, particularly at lower cyclic stress ratios (CSR = 0.15). In contrast, un-encased specimens typically failed within 20–50 cycles under similar loading conditions. At CSR = 0.15, encased samples often did not reach the failure threshold (either R_u=1.0 or DA strain ≥ 5%) even after 200 cycles, indicating substantial delay in pore pressure buildup and softening onset.

This improvement is attributed to the lateral confinement provided by the PET fabric, which limits radial expansion and helps maintain effective stress within the specimen during cyclic loading. The effect was more pronounced in loose specimens, where early mobilization of fabric tension occurred due to immediate lateral deformation. To simplify the resistance trend, Fig. 4(b) presents the normalized excess pore pressure ratio (R_u) behavior of the PET-encased specimens, plotted alongside reference boundaries derived using the Seed et al. (1975) formulation. These bounds represent the expected liquefaction behavior of clean Monterey sands, using the simplified relationship:

$$R_u = \frac{2}{\pi}\sin^{-1}\frac{N}{N_{liq}}^{\frac{1}{2\theta}}$$

where θ = 0.7 and 1.2 were used to define the upper and lower bounds of behavior based on range from Monterey Sands.

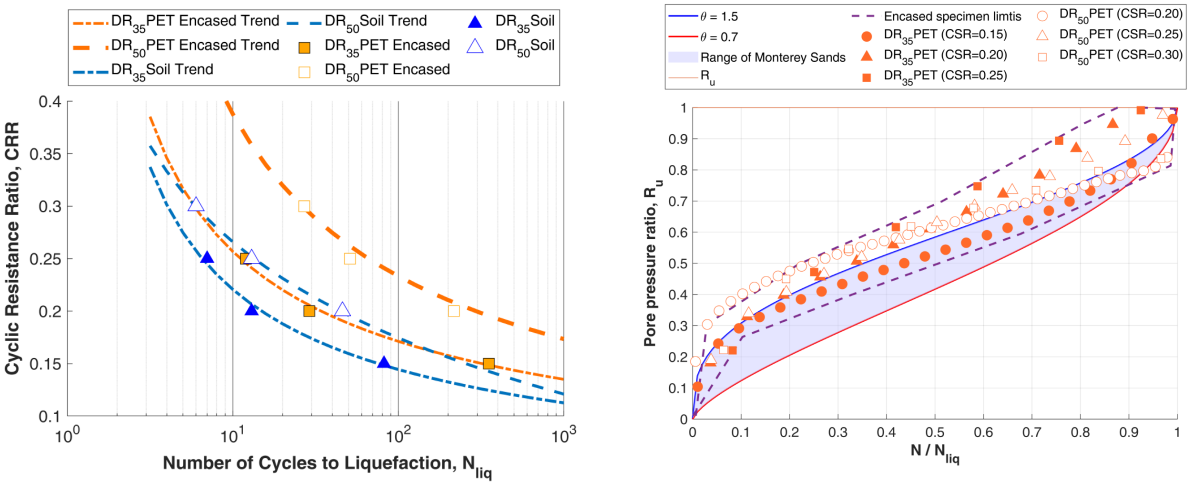

(a) (b)

Fig. 4(a) Cyclic resistance curve and (b) normalized pore pressure trend.

The encased specimen trends fall outside and above these bounds, indicating a delayed rate of pore pressure accumulation and extended resistance. This deviation from the Monterey sand baseline highlights the beneficial effect of encasement under undrained cyclic loading and supports the notion of apparent reinforcement and delayed softening. The trend also reflects the complex interaction between fabric confinement and evolving soil structure under repeated loading.

Principal Stress Rotation and Particle Rearrangement:

During cyclic loading, the PET-encased specimens exhibited a markedly different deformation behavior compared to un-encased soil. As shown in Fig. 5(a), axial strain accumulation progressed more gradually in encased specimens across all cyclic stress ratios (CSR). The double amplitude axial strain (DA) for PET-encased specimens (DA_{PET}) remained substantially lower than that of ordinary soil (DA_{OS}) at corresponding load levels. For example, at CSR = 0.25, DA_{PET} was limited to 1.45%, compared to 4.48% in the un-encased sample. Similar trends were observed at CSR = 0.20 (DA_{PET} = 0.54%, DA_{OS} = 3.56%) and CSR = 0.15 (DA_{PET} = 0.02%, DA_{OS} = 1.84%). This reduction confirms the role of geotextile encasement in restricting axial deformation by providing effective lateral confinement.

The evolution of normalized shear modulus (G/G_{max}) with respect to the number of cycles is shown in Fig. 5(b). PET-encased specimens retained a larger portion of their initial stiffness over extended cyclic loading, in contrast to ordinary soil, which exhibited more rapid stiffness degradation. Notably, the effect of relative density is clearly observed: at the same CSR, denser encased specimens (e.g., DR = 60%) preserved stiffness over more cycles than looser specimens (e.g., DR = 35%). This suggests that the beneficial impact of geotextile confinement becomes more amplified with increasing soil density, likely due to improved fabric-soil interlocking and reduced initial void ratio.

The improved modulus retention across densities indicates that the fabric mitigates particle rearrangement and delays the softening of the soil matrix. While direct stress path visualization (e.g., from advanced imaging or multiaxial loading) was not used, stress rotation was inferred from changes in deviator and confining stresses during cyclic loading. These inferred rotations, combined with the trends in strain suppression and stiffness preservation, point to a favorable redistribution of internal stresses within the encased specimens.

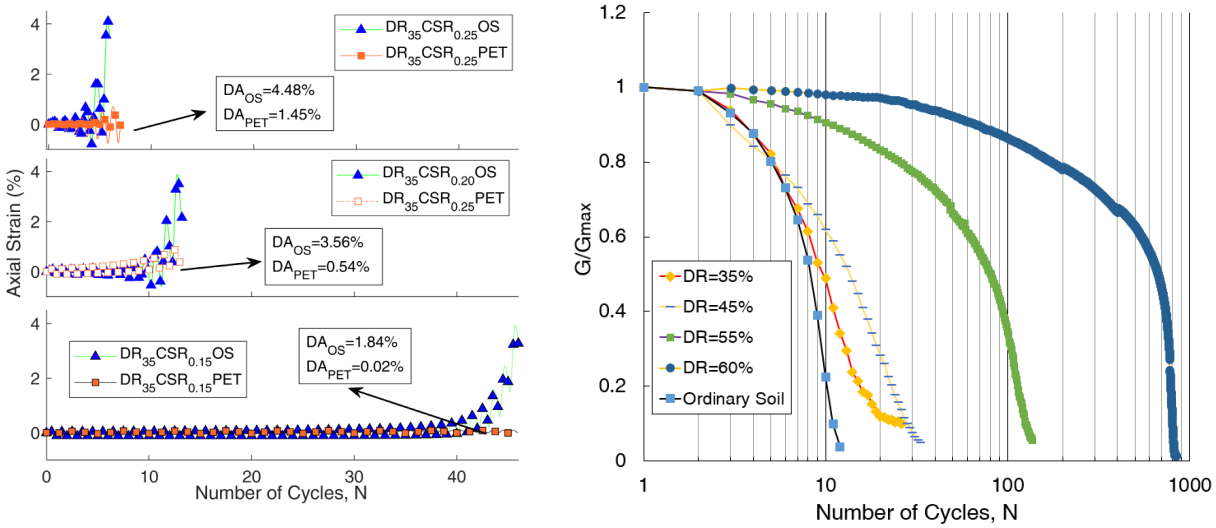

(a) (b)

Fig. 5(a) Axial strain vs number of cycles and (b) G/Gmax vs number of cycles.

Post Cyclic Behavior:

Following cyclic loading and full reconsolidation under drained conditions, PET-encased specimens were subjected to monotonic shearing to evaluate their residual strength and deformation characteristics. The results provide insights into how confinement influences recovery of mechanical performance after liquefaction-induced weakening. Fig. 6 illustrates the stress–strain response of a reconsolidated PET-encased specimen initially prepared at 50% relative density. Despite undergoing significant cyclic degradation, the specimen retained a stable and moderately stiff response during drained shearing. This suggests that the encasing fabric continued to provide structural confinement, even after cyclic strain softening and pore pressure dissipation.

The recovered strength behavior indicates two important phenomena:

- Preserved confinement function: Even after cyclic-induced rearrangement and stress reversal, the PET fabric maintained enough integrity that it still reinforces the fabric during monotonic shearing.
- Reconsolidated relative densities matches those reported by Green (2001) and Gohl et al. (2000).

Overall, the reconsolidated behavior reaffirms that geotextile confinement not only delays failure during cyclic loading but also supports partial recovery of strength by preserving internal structure during post-cyclic densification.

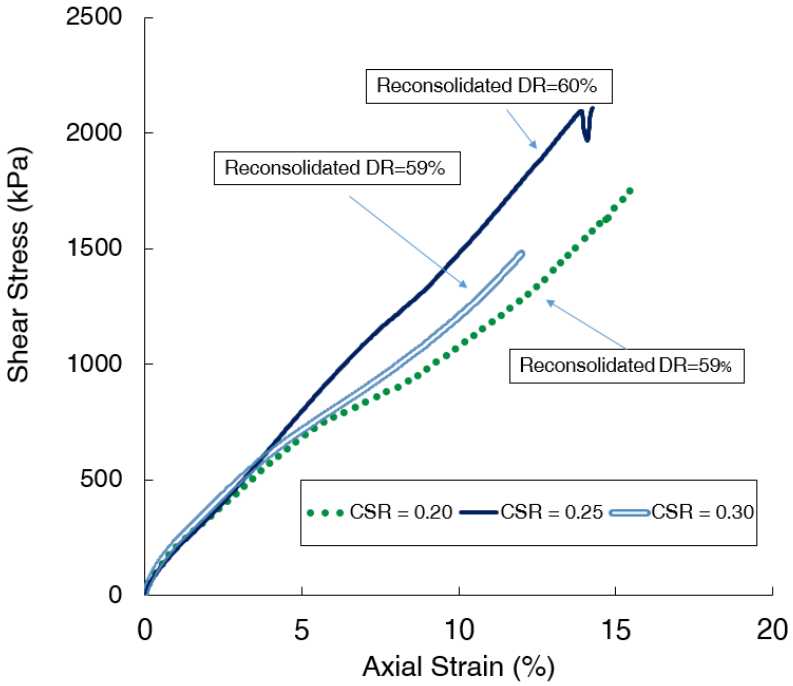

Fig. 6 Drained monotonic loading of reconsolidated encased specimens.

4. CONCLUSION

This study investigated the cyclic and post-cyclic behavior of PET-encased sand specimens under undrained triaxial loading conditions. The experimental results confirmed the beneficial role of geotextile confinement in enhancing liquefaction resistance and post-cyclic recovery.

- At a cyclic stress ratio (CSR) of 0.15, un-encased specimens typically failed within 20–50 cycles, while PET-encased specimens did not reach failure even after 200 cycles. At CSR = 0.20, PET encasement improved cyclic resistance by approximately 1.7–4.3 times, depending on the relative density. Double amplitude axial strains (DA) were also substantially reduced. For instance, at CSR = 0.25, the strain in PET-encased loose specimens was only 32.18% of that observed in un-encased counterparts, while in dense specimens the ratio was 18.95%.
- Normalized shear modulus trends (G/G_{max}) showed that PET encasement significantly delayed stiffness degradation across the number of cycles. After cyclic loading, reconsolidated specimens retained mechanical integrity and exhibited stable drained stress–strain responses. A PET-encased specimen initially prepared at 50% relative density reconsolidated at field values reported by Green (2001) and Gohl et al. (2000).
- These findings confirm that PET geotextile encasement improves both the cyclic stability and residual strength recovery of liquefiable soils. The improvements in cyclic resistance, strain suppression, and reconsolidated shearing response make geotextile encasement a reliable strategy for reinforcing soils in seismic and cyclically loaded environments.

ACKNOWLEDGEMENTS:

This research was supported by the Basic Science Research Program through the National Research Foundation of Korea (NRF) funded by the Ministry of Education (RS-2021-NR060134). Additionally, this work was supported by the Human Resources Development of the Korea Institute of Energy Technology Evaluation and Planning(KETEP) grant funded by the Korea government Ministry of Trade, Industry & Energy (No. RS-2021-KP002506).

REFERENCES:

ASTM International. (2013). *ASTM D5311M-13: Standard test method for load controlled cyclic triaxial strength of soil*. https://www.astm.org/d5311m-13.html

Frost, J. D., & Park, J. Y. (2003). A critical assessment of the moist tamping technique. *Geotechnical testing journal*, *26*(1), 57-70.

Gohl, W. B., Jefferies, M. G., Howies, J. A., & Diggle, D. (2000). Explosive compaction: design, implementation and effectiveness. *Geotechnique*, *50*(6), 657-665.

Green, R. A., & Mitchell, J. K. (2004). Energy-based evaluation and remediation of liquefiable soils. In *Geotechnical engineering for transportation projects* (pp. 1961-1970).

Ishihara, K., & Yoshimine, M. (1992). Evaluation of settlements in sand deposits following liquefaction during earthquakes. *Soils and foundations*, *32*(1), 173-188.

Kim, H. J., Dinoy, P. R., Reyes, J. V., Kim, H. S., Park, T. W., & Choi, H. S. (2023). Seismic Characteristics of a Geotextile Tube-Reinforced Embankment and Shallow Foundations Laid on Liquefiable Soil. *Applied Sciences*, *13*(2), 785.

Ladd, R. S. (1978). Preparing test specimens using undercompaction. *Geotechnical testing journal*, *1*(1), 16-23.

Miranda, M., Da Costa, A., Castro, J., & Sagaseta, C. (2017). Influence of geotextile encasement on the behaviour of stone columns: Laboratory study. *Geotextiles and Geomembranes*, *45*(1), 14-22.

Raithel, M., Kempfert, H. G., & Kirchner, A. (2002, September). Geotextile-encased columns (GEC) for foundation of a dike on very soft soils. In *Proc., 7th Int. Conf. on Geosynthetics* (Vol. 3, pp. 1025-1028). Nice, France: Swets & Zeitlinger.

Seed, H. B., Martin, P. P., & Lysmer, J. (1975). *The generation and dissipation of pore water pressures during soil liquefaction*. College of Engineering, University of California.

Youd, T. L., & Idriss, I. M. (2001). Liquefaction resistance of soils: summary report from the 1996 NCEER and 1998 NCEER/NSF workshops on evaluation of liquefaction resistance of soils. *Journal of geotechnical and geoenvironmental engineering*, *127*(4), 297-313.

Yoo, C., & Abbas, Q. (2020). Laboratory investigation of the behavior of a geosynthetic encased stone column in sand under cyclic loading. *Geotextiles and Geomembranes*, *48*(4), 431-442.

Zhu, Z., Zhang, F., Peng, Q., Dupla, J. C., Canou, J., Cumunel, G., & Foerster, E. (2021). Effect of the loading frequency on the sand liquefaction behaviour in cyclic triaxial tests. *Soil dynamics and earthquake engineering*, *147*, 106779.